Analysis of the Triaxial Test—Cohesionless Soils

Analyse de l'essai triaxial—sols pulvérulents

B. B. BROMS, PH.D., *Associate Professor of Civil Engineering, Cornell University, Ithaca, U.S.A.*
A. K. JAMAL, B.SC.(Dunelm), M.S., *Aggrey Fellow, Cornell University, Ithaca, U.S.A.*

SUMMARY

Solid and hollow samples of a cohesionless soil have been tested to failure under undrained conditions. For some of the hollow specimens, volume changes of the inside chamber were prevented. By measuring the inside chamber pressure, it has been possible to measure directly the corresponding radial stress in a solid sample.

The test data indicate that for cohesionless soils the standard triaxial test will underestimate the angle of internal friction ϕ' by approximately 3 to 4 degrees when the relative density is high while at medium to low relative densities, the friction angle ϕ' determined from standard triaxial tests will correspond to its maximum possible value. A difference in the friction angle ϕ' of 3 to 4 degrees is sufficient to explain the difference observed by a number of investigators for dense sand between extension and compression tests and between the calculated and measured bearing capacity of model footings.

SOMMAIRE

Des échantillons creux et pleins d'un sol sans cohésion ont été examinés dans des conditions non-drainées. Pour une partie des échantillons creux, les changements de volume de la chambre intérieure furent empêchés. En mesurant la pression de la chambre intérieure il fut possible de mesurer directement la contrainte radiale correspondante dans un échantillon plein.

Les résultats des épreuves indiquent que pour des sols sans cohésion les essais triaxiaux sous-estiment l'angle de friction interne ϕ' d'environ 3 à 4 degrés quand la densité relative est forte; pour des densités intermédiaires et faibles, l'angle de friction ϕ' déterminé par des essais triaxiaux correspond à sa valeur maximale. Une différence de 3 à 4 degrés dans l'angle de friction est suffisante pour expliquer la différence observée par plusieurs chercheurs dans le cas d'un sable dense entre des épreuves de tension et de compression et entre la force portante calculée et mesurée pour les semelles modèles.

IN THE ANALYSIS of the standard triaxial compression test, it is generally assumed that the stresses within the soil specimen are uniformly distributed and that the intermediate principal stress is equal to the minor principal stress. The test results are usually analysed by the Coulomb-Mohr failure criterion and the shear strength of the soil is expressed in terms of an angle of internal friction ϕ and a cohesion c.

For cohesionless soils the angle of internal friction ϕ' with respect to effective stresses as measured by axial compression tests has been found by several investigators to be lower than that measured by axial extension tests (Taylor, 1941; Habib, 1953; Peltier, 1957; Henkel, 1959; Haythornthwaite 1960) or that measured under the condition of plane strain (Bishop, 1961; Whitman and Luscher, 1962). On the other hand, Bishop and Eldin (1953) and Kirkpatrick (1957) have found close agreement between compression and extension tests.

Experiments by Hansen (1961) and by Tcheng (1957) have indicated that the bearing capacity of model footings placed on dense sand may exceed considerably that predicted by existing bearing capacity theories if the shear-strength parameters determined from standard triaxial compression tests are used in the analysis of the test data. However, close agreement was found for footings located on medium to loose sand.

The observed differences between compression and extension tests and between compression tests and tests carried out under the condition of plane strain can be attributed to a non-uniform stress distribution within the standard triaxial test specimen as will be shown by the investigation described in this paper. This non-uniform stress distribution can also explain the observed differences between measured and calculated bearing capacity which have been observed for model footings placed on dense sand.

STRESS DISTRIBUTION WITHIN TRIAXIAL TEST SPECIMEN

In a standard triaxial compression test, the major principal stress, σ_z, acts in the direction of the axis of the test specimen. Its average value, $(\sigma_z)_{av}$ is equal to P/A where P is the applied axial load and A is the cross-sectional area. The radial stress, σ_r, and the circumferential stress, σ_θ, (defined in Fig. 1) may be either the intermediate or the minor

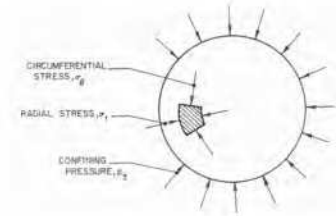

FIG. 1. Circumferential and radial stresses.

principal stress. The stress distribution when the radial stress increases toward the centre of the test specimen is shown in Fig. 2a and the stress distribution when the radial stress decreases toward the centre is shown in Fig. 2b.

The average circumferential stress $(\sigma_\theta)_{av}$ can be calculated from equilibrium conditions and is equal to the applied confining pressure, p_3. The radial stress, σ_r, is equal to the confining pressure p_3 at the surface of the test member specimen (Fig. 2). For the case (case I) when the radial stress increases toward the centre of the test specimen, the average radial stress $(\sigma_r)_{av}$ will be larger than the confining pressure p_3; while for the case (case II) when the radial stress decreases toward the centre, its average value will be less than the confining pressure p_3.

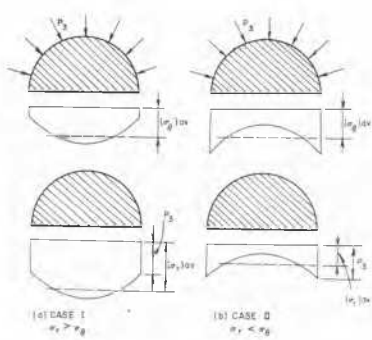

FIG. 2. Stress distribution.

Mohr's stress circles corresponding to the two cases are shown in Fig. 3. The shear-strength parameters ϕ and c are generally determined by constructing the envelope curve to a series of stress circles governed by the average axial stress (P/A) at failure and the confining pressure p_3. For case I, the shear strength parameters ϕ and c will be equal to ϕ_a and c_a, whereas for case II, these parameters will be equal to ϕ_b and c_b. The friction angle ϕ_b and the cohesion c_b, corresponding to the major and the intermediate principal stresses, may be considerably smaller than the shear-strength parameters ϕ_a and c_a corresponding to the major and minor principal stresses.

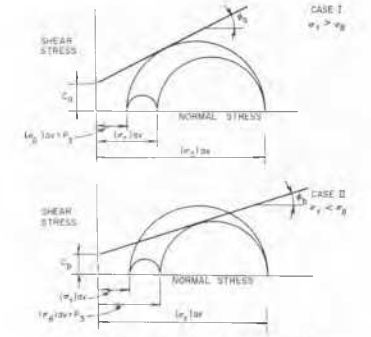

FIG. 3. Interpretation of triaxial tests.

In the case when the radial stress decreases towards the centre, the angle of internal friction will correspond to the major and the intermediate principal stresses rather than the major and minor principal stresses. For this case, the standard triaxial test will underestimate the angle of internal friction.

OUTLINE OF TEST PROGRAMME

In a standard triaxial test specimen, all radial planes are planes of symmetry and the shear stresses on these planes will at all times be equal to zero. Since the shear stresses on two perpendicular planes are always equal, the shear stress on any circumferential plane will be equal to zero, the latter being perpendicular to the radial planes. Therefore, the shear stress will be equal to zero on the plane corresponding to the inside surface of a hollow cylindrical specimen with the same outside dimensions as those of the corresponding solid specimen. The centre core of a solid specimen may therefore be replaced by a liquid and in this case, the shear stress along the inside face of the resulting hollow specimen will also be equal to zero.

Furthermore, the liquid will have the same deformation characteristics (it is incompressible) as the saturated soil it replaces if volume changes are prevented in the hollow specimen. Thus, by measuring the changes in the inside chamber pressure for the hollow specimen, the corresponding changes in the radial stress can be measured directly for the standard solid triaxial specimen.

In order to investigate the hypothesis presented above, three series of consolidated-undrained tests were carried out on a beach sand at different relative densities. In series I, solid samples with a diameter of 3.0 in. and a height of 6.0 in. were tested while in series II and III, hollow cylindrical samples with a height of 12.0 in. and with outside and inside diameters of 6.0 and 3.0 in., respectively, were tested. The inside chamber pressure was kept constant in series II. In this series, volume changes of the inside chamber were allowed. The volume of the inside chamber was kept constant in series III and the resulting changes of the inside chamber pressure were measured. All tests were carried out at a constant axial strain rate of 0.1 per cent per minute.

MATERIAL AND TEST APPARATUS

A beach sand consisting of rounded quartz particles of a high degree of purity was used in this investigation. The grain size ranged from 0.8 mm to 0.1 mm. The coefficient of uniformity of the sand was 1.67 and its effective grain size was 0.18 mm. The specific gravity of the quartz particles was 2.65 and the maximum and minimum porosities of the sand were 0.50 and 0.36, respectively (Kolbuszewski, 1948).

A standard cell was used for the solid specimens tested in series I. A modified triaxial cell was utilized for series II and III. The hollow cylindrical test specimen was sealed between an inner and an outer rubber membrane and between two ring plates. Pressure changes in the inside chamber of the hollow specimens (series III) were measured by a simple differential mercury manometer, volume changes being prevented by means of a null indicator and a back pressure system.

TEST PROCEDURE

The sand used in this investigation was boiled before moulding in order to ensure a maximum degree of saturation. Different compaction procedures were used to vary the relative density of the sand. To obtain a medium to low relative density (Meyerhof, 1956), the sand was placed under water in three layers and each layer was rodded lightly. For a relative density ranging from medium to dense, the sand was placed under water and vibrated for 5, 15, or 30 seconds on a vibrating table. By such a procedure, the porosity could be varied between 0.36 and 0.44 for the solid samples and between 0.38 and 0.46 for the thin-walled hollow samples.

The specimens were allowed to consolidate fully at a confining pressure of 7.1 or 14.2 lb/sq. in. whereafter a back pressure was applied to ensure full saturation. By increasing the confining pressure slightly and by measuring the resulting pore-pressure increase, the degree of saturation of the test specimens could be checked. The test specimens were then tested to failure under undrained conditions and under increasing axial load. The resulting pore-pressure changes were measured.

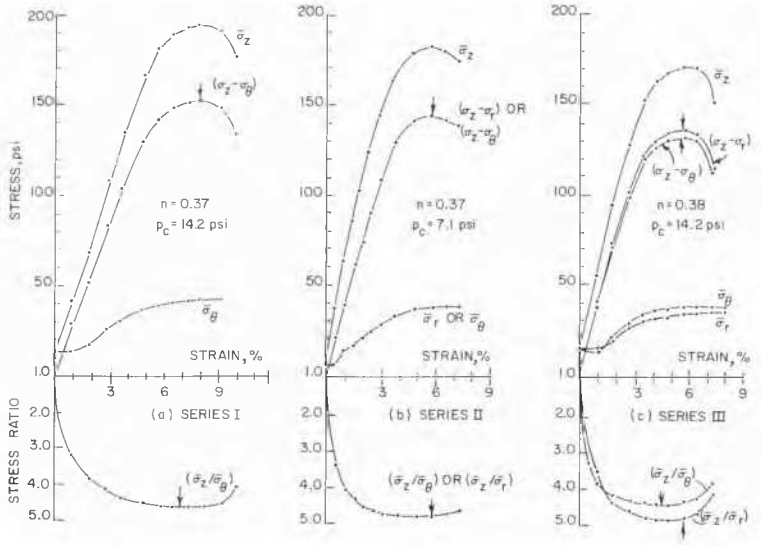

FIG. 4. Typical stress-strain relationships—high relative density.

TEST RESULTS

Stress-Strain Relationships

Typical stress-strain relationships as obtained from the solid samples (series I), the hollow samples where volume changes of the inside chamber were allowed (series II), and the hollow samples where no volume changes of the inside chamber were allowed (series III) are shown in Figs. 4 and 5. The relationships shown in Fig. 4 are those for specimens at a high relative density (corresponding low porosity) while those shown in Fig. 5 were obtained for specimens having medium to low relative density (medium to high porosity).

For the solid specimens, the maximum principal stress ratio $(\bar{\sigma}_z/\bar{\sigma}_\theta)_{max}$ was reached at an axial strain which was smaller than that corresponding to the maximum deviator stress $(\sigma_z - \sigma_\theta)$ as shown in Fig. 4a, while for the solid samples with a medium relative density, the strains corresponding to $\bar{\sigma}_z/\bar{\sigma}_\theta)_{max}$ and to $(\sigma_z - \sigma_\theta)_{max}$ were approximately the same (Fig. 5a). The strains corresponding to $\bar{\sigma}_z/\bar{\sigma}_r)_{max}$ or $(\sigma_z - \sigma_r)_{max}$ were, as shown in Figs. 4b and 5b, approximately the same for the hollow samples where volume changes of the inside chamber were allowed (series II) regardless of the initial porosity of soil.

For the hollow samples at high relative density where volume changes of the inside chamber were prevented

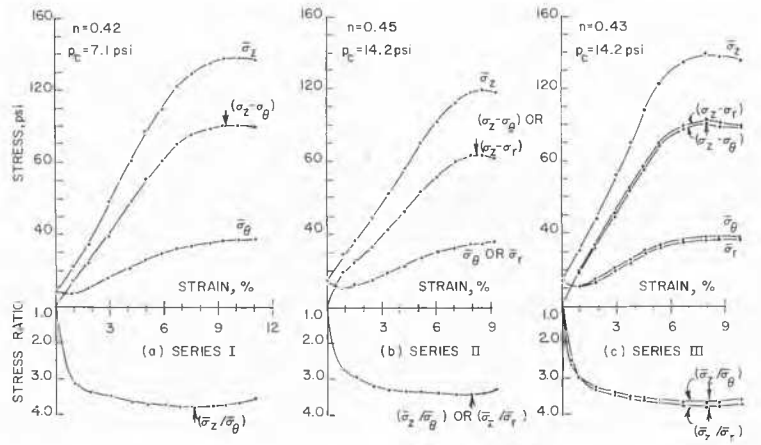

FIG. 5. Typical stress-strain relationships—low relative density.

(series III), the maximum principal stress ratio $(\bar{\sigma}_z/\bar{\sigma}_\theta)_{max}$ with respect to the average effective circumferential stress was reached at a strain less than that corresponding to the maximum deviator stress $(\sigma_z - \sigma_\theta)_{max}$. The strain corresponding to $(\sigma_z/\sigma_\theta)_{max}$ was approximately equal to that measured for the solid samples (Fig. 4a).

It can be seen from Fig. 4c that for series III, the strain corresponding to $(\bar{\sigma}_z/\bar{\sigma}_r)_{max}$ is approximately equal to that corresponding to $(\sigma_z - \sigma_r)_{max}$. This strain is approximately equal to that corresponding to $(\bar{\sigma}_z/\bar{\sigma}_r)_{max}$ as obtained for the hollow samples tested in series II (Fig. 4b). For the samples with a medium to low relative density in series III (Fig. 5c), the strains corresponding to $(\bar{\sigma}_z/\bar{\sigma}_\theta)_{max}$ and to $(\bar{\sigma}_z/\bar{\sigma}_r)_{max}$ are approximately the same. These strains compare well with those measured for series I and II (Figs. 5a and 5b).

From the stress-strain relationships in Figs. 4c and 5c (series III), it can be noted that the circumferential effective stress $(\bar{\sigma}_\theta)_{av}$ is smaller than the radial stress $(\bar{\sigma}_r)_{av}$ at axial unit deformation less than about 2 per cent, while at larger deformations, the circumferential stress is larger than the radial stress. Thus, the circumferential stress is the minor principal stress at small axial deformations while at relatively large axial deformations, the radial stress is the minor principal stress.

Friction Angle ϕ'

For series III (Fig. 4c), the ratio $(\bar{\sigma}_z/\bar{\sigma}_\theta)_{max}$ is smaller than the ratio $(\bar{\sigma}_z/\bar{\sigma}_r)_{max}$, thus indicating that for dense sand, the friction angle ϕ' corresponding to the axial and the radial stresses is larger than that corresponding to the axial and the circumferential stresses. For the hollow specimens tested at low relative density (Fig. 5c) the difference between the stress ratios $(\bar{\sigma}_z/\bar{\sigma}_\theta)_{max}$ and $(\bar{\sigma}_z/\bar{\sigma}_r)_{max}$ is small and the maximum values of these stress ratios occurred approximately at the same axial unit deformation. Thus, for this case, the friction angle ϕ' corresponding to the axial and the circumferential stresses is approximately equal to that corresponding to the axial and the radial stresses.

The shape of the stress-strain relationships and differences between the $(\bar{\sigma}_z/\bar{\sigma}_\theta)_{max}$ and $(\bar{\sigma}_z/\bar{\sigma}_r)_{max}$ observed for series III indicate that the standard triaxial test tends to underestimate the shear-strength parameter ϕ' at high relative densities of the cohesionless soils, while at medium or low relative densities, the standard triaxial test will give a true indication of this shear-strength parameter.

Relationship between Porosity and Friction Angle ϕ'

Since the porosity varied slightly between the individual tests and between the hollow and the solid specimens, a direct comparison between series I, II, and III cannot be made. In order to correct for differences in porosity, the calculated friction angle ϕ' corresponding to either $(\bar{\sigma}_z/\sigma_r)_{max}$ or to $(\bar{\sigma}_z/\bar{\sigma}_\theta)_{max}$ has been plotted in Fig. 6 as a function of the initial porosity of the samples.

It can be seen that the friction angle ϕ' corresponding to $(\bar{\sigma}_z/\bar{\sigma}_\theta)_{max}$ determined from series III is approximately equal to that determined from the standard trixial test specimen (the solid samples) and that the friction angle ϕ' at $(\bar{\sigma}_z/\bar{\sigma}_r)_{max}$ corresponds closely to that determined from series II. The difference between the two values of the friction angle ϕ' is about 3 to 4 degrees at a high relative density, and this difference decreases with decreasing relative density (increasing porosity). The difference is relatively small at medium and low relative densities.

A difference of 3 to 4 degrees in the friction angle ϕ' is sufficient to account for the differences observed between the extension and compression tests and for the difference observed between measured and calculated bearing capacity of model footings.

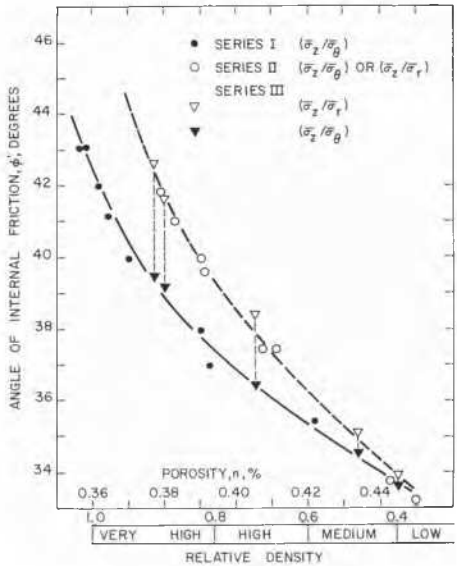

FIG. 6. Relationships between friction angle ϕ' and porosity.

ACKNOWLEDGMENT

This investigation has been supported by the National Science Foundation (Grant No. G-21833).

REFERENCES

BISHOP, A. W. (1961). Discussion, Section I. *Proc. Fifth International Conference on Soil Mechanics and Foundation Engineering*, Vol. 3, pp. 97–100.

BISHOP, A. W., and A. K. G. ELDIN (1953). The effect of stress history on the relation between ϕ and porosity in sand. *Proc. Third International Conference on Soil Mechanics and Foundation Engineering*, Vol. 1, pp. 100–5.

HABIB, P. (1953) Influence de la variation de la contrainte principale moyenne sur la résistance au cisaillement des sols. *Proc. Third International Conference on Soil Mechanics and Foundation Engineering*, Vol. 1, pp. 131–6.

HANSEN, B. (1961). The bearing capacity of sand, tested by loading circular plates. *Proc. Fifth International Conference on Soil Mechanics and Foundation Engineering*, Vol. 1, pp. 659–64.

HAYTHORNTHWAITE, R. M. (1960). Mechanics of the triaxial test for soils. *Proc. American Society of Civil Engineers*, Vol. 86, No. SM5, Paper 2625, pp. 35–62.

HENKEL, D. J. (1959). The relationships between the strength, pore water pressure and volume change characteristics of saturated clays. *Géotechnique*, Vol. 9, pp. 119–35.

KIRKPATRICK, W. M. (1957). The condition of failure for sands, *Proc. Fourth International Conference on Soil Mechanics and Foundation Engineering*, Vol. 1, pp. 172–8.

KOLBUSZEWSKI, J. J. (1948). An experimental study of the

maximum and minimum porosities of sands. *Proc. Second International Conference on Soil Mechanics and Foundation Engineering*, Vol. 1, pp. 158–65.

MEYERHOF, G. G. (1956). Penetration tests and bearing capacity of cohesionless soils. *Proc. American Society of Civil Engineers*, Vol. 82, No. SM1, Paper 866, pp. 1–19.

PELTIER, M. R. (1957). Experimental investigations of the intrinsic rupture curve of cohesionless soils. *Proc. Fourth International Conference on Soil Mechanics and Foundation Engineering*. Vol. 1, pp. 179–82.

TAYLOR, D. W. (1941). Seventh Progress Report on Shear Research to U.S. Corps of Engineers. MIT Publication, Cambridge, Mass.

TCHENG, Y. (1957). Fondations superficielles en milieu stratifié. *Proc. Fourth International Conference on Soil Mechanics and Foundation Engineering*, Vol. 1, pp. 449–52.

WHITMAN, R. V. and U. LUSCHER (1962). Basic experiment into soil-structure interaction. *Proc. American Society of Civil Engineers*, Vol. 88, No. SM6, pp. 135–67.